A new type of scorpion Na^+-channel-toxin-like polypeptide active on K^+ channels

Najet SRAIRI-ABID*[1], Joseba Iñaki GUIJARRO†[2], Rym BENKHALIFA*[2], Massimo MANTEGAZZA‡, Amani CHEIKH*, Manel BEN AISSA†, Pierre-Yves HAUMONT§, Muriel DELEPIERRE† and Mohamed EL AYEB*

*Laboratoire des Venins et Toxines, Institut Pasteur de Tunis, 13, place Pasteur, BP-74 Tunis 1002, Tunisia, †Unité de RMN des Biomolécules, Dépt. de Biologie Structurale et Chimie, Institut Pasteur (CNRS URA 2185), 28 rue du Docteur Roux, 75724 Paris Cedex 15, France, ‡Cellular Neurophysiology Laboratory, Istituto Neurologico, Besta Via Libero Temolo 4, 20126 Milano, Italy, and §Société Applied Biosystems, 25 avenue de la Baltique, BP 96, 91943 Courtaboeuf Cedex, France

We have purified and characterized two peptides, named KAaH1 and KAaH2 (AaH polypeptides 1 and 2 active on K^+ channels, where AaH stands for *Androctonus australis* Hector), from the venom of *A. australis* Hector scorpions. Their sequences contain 58 amino acids including six half-cysteines and differ only at positions 26 (Phe/Ser) and 29 (Lys/Gln). Although KAaH1 and KAaH2 show important sequence similarity with anti-mammal β toxins specific for voltage-gated Na^+ channels, only weak β-like effects were observed when KAaH1 or KAaH2 (1 μM) were tested on brain Nav1.2 channels. In contrast, KAaH1 blocks Kv1.1 and Kv1.3 channels expressed in *Xenopus* oocytes with IC_{50} values of 5 and 50 nM respectively, whereas KAaH2 blocks only 20 % of the current on Kv1.1 and is not active on Kv1.3 channels at a 100 nM concentration. KAaH1 is thus the first member of a new subfamily of long-chain toxins mainly active on voltage-gated K^+ channels. NMR spectra of KAaH1 and KAaH2 show good dispersion of signals but broad lines and poor quality. Self-diffusion NMR experiments indicate that lines are broadened due to a conformational exchange on the millisecond time scale. NMR and CD indicate that both polypeptides adopt a similar fold with α-helical and β-sheet structures. Homology-based molecular models generated for KAaH1 and KAaH2 are in accordance with CD and NMR data. In the model of KAaH1, the functionally important residues Phe^{26} and Lys^{29} are close to each other and are located in the α-helix. These residues may constitute the so-called functional dyad observed for short α-KTx scorpion toxins in the β-sheet.

Key words: *Androctonus australis* scorpion, dyad F/K, K^+ channel, Na^+ channel, scorpion toxin, structure–function relationship.

INTRODUCTION

Scorpion venoms are mixtures of numerous neurotoxins [1,2] and other non-toxic peptides [3–6]. These neurotoxins can be classified as either long- or short-chain toxins. Most long-chain toxins are composed of 60–70 residues and are cross-linked by four disulphide bridges [7]. These target voltage-gated Na^+ channels and can be classified into α-toxins, which slow down Na^+ channel inactivation, and β-toxins, which affect the channel activation process [8]. Short-chain toxins usually contain 30–40 residues and three or four disulphide bridges. Most of the short-chain toxins described to date block voltage-dependent or Ca^{2+}-activated K^+ channels. Short and long toxins share a common structural motif [9], named CS-α/β for cysteine-stabilized α-helix/β-sheet. Recently, a novel type of scorpion toxin was isolated from the South African scorpion *Parabuthus transvaalicus*: birtoxin and ikitoxin. These are composed of 58 amino acids and contain six cysteines in contrast with the eight cysteines present in all other known long-chain scorpion toxins [10,11]. Both toxins are active against mice when administered intracerebroventricularly and are classified as β-toxins active on voltage-gated Na^+ channels from central neurons. We have purified two polypeptides from AaH (*Androctonus australis* Hector) scorpions, KAaH1 and KAaH2 (AaH polypeptides 1 and 2 active on K^+ channels), which show approx. 60 % identity (~70 % similarity) with birtoxin and ikitoxin. Despite this important sequence identity, KAaH1 and KAaH2 show different biological characteristics. In the present study, we describe the activity and the structural characterization of both polypeptides that define a new type of scorpion venom proteins.

EXPERIMENTAL

Scorpion venom

Venom of *A. australis* Hector scorpions from Beni Khedach (Tunisia) was collected by the veterinarian service of the Pasteur Institute of Tunisia and kept frozen at −20 °C in its crude form until use. Chemicals (reagent grade) were purchased from Sigma, unless indicated otherwise.

Purification of KAaH1 and KAaH2

Crude venom was dissolved in water and loaded on Sephadex G-50 gel filtration chromatography columns (2 × K26/100) to isolate the toxic fraction, named AaHG50. Columns were equilibrated with 0.1 M acetic acid. After freeze-drying, the AaHG50 fraction was fractionated by FPLC on a Mono S HR 5/5 column pre-equilibrated with 0.1 M ammonium acetate buffer (pH 8.5). Proteins were eluted with a 30 min linear gradient from 0.1 to 0.5 M ammonium acetate (pH 8.5) at a flow rate of 1 ml/min. Absorbance was monitored at 280 nm.

HPLC purification of the non-retained fraction was performed using a C8 reversed-phase HPLC column (5 μm, 4.6 × 250 mm;

Abbreviations used: AaH, *Androctonus australis* Hector; KAaH1 and KAaH2, AaH polypeptides 1 and 2 active on K^+ channels; MBS, modified Barth's saline; TFA, trifluoroacetic acid.

[1] To whom correspondence should be addressed (email najet.abid@pasteur.rns.tn).

[2] These authors have contributed equally to this work.

Beckman, Fullerton, CA, U.S.A.), equipped with a Beckman Series 125 pump and a Beckman diode array detector set at 214 and 280 nm. Elution was controlled by means of the software GOLD. Proteins were eluted from the column at the rate of 1 ml/min using a linear gradient (25 min) from 20 to 40 % of solution B [0.1 % TFA (trifluoroacetic acid) in acetonitrile] in solution A (0.1 % TFA in water).

In vivo toxicity tests

The *in vivo* toxicity of KAaH1 and KAaH2 was tested on 20 ± 2 g male C57/BL6 mice by intracerebroventricular injection of 5 μl of 0.1 % BSA solutions containing increasing amounts of the polypeptides. Six mice were used for each concentration.

Electrophysiological characterization

Activity on K^+ channels

Mature female *Xenopus laevis* were anaesthetized by immersion in a 0.17 % solution of tricaine (ethyl *M*-aminobenzoate). Ovarian lobes were surgically isolated and rinsed in standard MBS (modified Barth's saline) of the following composition: 88 mM NaCl, 1 mM KCl, 2.4 mM $CaCl_2$, 0.82 mM $MgSO_4$, 2.4 mM $NaHCO_3$, 0.41 mM $MgCl_2$, 0.33 mM $Ca(NO_3)_2$, 10 mM Hepes (pH 7.4).

Stage V–VI oocytes were defolliculated by collagenase treatment (type A and type B; Boehringer, Mannheim, Germany; 2 mg/ml in calcium-free MBS), then mechanically using two thin forceps.

Rat Kv1.1 and Kv1.3 cRNAs (gifts from Dr M. Crest, Laboratoire Intégration des Informations Sensorielles, CNRS, Marseille, France) were stored at 1 μg/ml in diethyl pyrocarbonate-treated water and injected at a concentration of 4 ng/oocyte using an automatic injector (Drummond Nanoject, Polylabo, France). Oocytes were incubated at 16–18 °C in sterile MBS supplemented with 0.1 mM gentamicin (Sigma).

Ionic currents through the Kv1.1 and Kv1.3 channels were recorded during the week following RNA injection with the two-electrode voltage-clamp method using a Gene Clamp 500 amplifier (Axon Instruments, Foster City, CA, U.S.A.).

Oocytes were immersed in calcium-free saline and impaled with two glass intracellular electrodes filled with 3 M KCl. The resistance of the pulled electrodes (P-97 puller; Sutter Instruments, Novato, CA, U.S.A.) was 1–2 MΩ. The holding potential was set at ± 80 mV. The perfusion system was controlled by a Manifold Solution Changer (MSC-200, Bio-Logic, France). Data acquisition and analysis were performed using Clampex and Clampfit from Pclamp8 software (Axon Instruments). Leak and capacitive currents were subtracted during analysis using a P/4 or P/8 method.

Activity on Na^+ channels

The tsA-201 cell subclone of HEK-293 cells was maintained at 37 °C in 10 % CO_2 in Dulbecco's modified Eagle's medium/F12 medium supplemented with 10 % (v/v) foetal bovine serum (Invitrogen). The cells were transiently co-transfected with rat cDNAs for the channel α subunits (plasmids pCDM8-rNav1.2a or pCDM8-rNav1.5, gifts from Dr William Catterall, Department of Pharmacology, University of Washington, Seattle, WA, U.S.A.) and the vector pEGFP-N1 (encoding the enhanced green fluorescent protein; ClonTech Ozyme, Saint Quentin en Yvelines, France) using calcium phosphate precipitation. Transfected cells were identified by fluorescence. Whole-cell patch–clamp recordings were performed at room temperature (22–25 °C) by using a Multiclamp 700 A amplifier (Axon Instruments) with PCLAMP 8 software (Axon Instruments). Capacitative currents were minimized by the amplifier circuitry, and 80–85 % prediction and series resistance compensation were routinely used. The remaining linear capacity and leakage currents were eliminated by P/4 subtraction. The extracellular solution contained (mM): 140 NaCl, 2 $CaCl_2$, 2 $MgCl_2$ and 10 Hepes (pH 7.4) adjusted with NaOH. The intracellular solution contained (mM): 195 *N*-methyl-D-glucamine, 10 NaCl, 4 $MgCl_2$, 10 Hepes and 5 EGTA (pH 7.2) adjusted with H_3PO_4. The toxins were either applied by perfusion (at the concentration of 100 nM) or placed directly in the bath extracellular solution before the beginning of the recordings (at the concentration of 1 μM).

Current–voltage (I–V) relationships were measured with depolarizing pulses from -80 to 20 mV in 5 mV steps (holding potential -100 mV) for Nav1.2a, and with pulses from -120 to 0 mV in 5 mV steps (holding potential -120 mV) for Nav1.5. Conductance–voltage ($g-V$) relationships (activation curves) were calculated from the $I-V$ relationships according to $g = I_{Na}/(V - E_{Na})$, where I_{Na} is the peak Na^+ current measured at potential V and E_{Na} is the calculated equilibrium potential. Inactivation curves were measured with a holding potential of -100 mV (Nav1.2a) or -120 mV (Nav1.5), applying 100 ms preconditioning steps from -100 to 0 mV for Nav1.2a, and from -120 to 0 mV for Nav1.5, followed by a test pulse to -10 mV (Nav1.2a) or -20 mV (Nav1.5). To evaluate the effects of the toxins, methods with a 1 ms prepulse to $+60$ mV applied 60 ms before the test were also used. Normalized activation and inactivation curves were fitted to a single or to a sum of two Boltzmann relationships of the form $y = 1/\{1 + \exp[(V_{1/2} - V)/k]\}$, where $V_{1/2}$ is the voltage (in mV) of half-maximal activation (Va) or inactivation (Vh), and k is a slope factor (mV).

Amino acid sequence determination

Reduction and alkylation of proteins, and sequence determination of native and S-alkylated peptides were performed as described in [6].

MS

Samples were analysed on Voyager-DE™ PRO MALDI-TOF Workstation (Applied Biosystems, Framingham, MA, U.S.A.) and triple quadrupole electrospray API 365 (Applied Biosystems/MDS-SCIEX, Concord, Ontario, Canada) spectrometers using standard techniques.

NMR

The purified peptides were freeze-dried, dissolved in 180 μl of 5 mM $C[^2H_2]_3CO_2Na$, 10 % ^2H_2O, pH 4.0 (buffer A), and centrifuged at 17 600 ***g*** for 20 min at 4 °C to remove any eventual aggregate. The concentration of the peptides in 3 mm Shigemi tubes (Shigemi, Allison Park, PA, U.S.A.) was 0.42 mM. For experiments in ^2H_2O, the samples were freeze-dried and dissolved in the same volume of ^2H_2O to obtain the same salt concentration as compared with samples before freeze-drying. Alternatively, for diffusion experiments (see below), the freeze-dried polypeptides were dissolved directly in buffer A prepared in ^2H_2O.

NMR experiments were run on Inova spectrometers (Varian, Palo Alto, CA, U.S.A.) resonating at 599.9 or 499.8 MHz ^1H frequencies. The spectrometers were equipped with 5 mm bore diameter pulse-field gradient probes. Vnmr 6.1C (Varian) and NMRView 5.0.3 [12] were used for acquisition, data processing and analysis. Experiments were performed at 5, 15, 25 or 35 °C. Chemical shifts are referenced to the sodium salt of 4,4 dimethyl-4-silapentane sulphonate.

Spectra were acquired with a spectral width of 11.5 p.p.m. The intensity of the water signal was decreased either by presaturation during the recycle delay or using the Watergate pulse scheme [13,14]. Homonuclear ^1H two-dimensional spectra were acquired with typically 32, 48 or 64 scans per increment, 400–512 increments on the indirect dimension, and a 2.2 s recycle delay. Purged COSY spectra were obtained as described in [15]. TOCSY spectra were run with a mixing time of 70 or 80 ms [16]. Spins were locked using the MLEV-17 sequence [17,18]. NOESY spectra were acquired with a mixing time of 150 ms [19].

NMR diffusion experiments were performed at 25 °C using the GCSTESL (gradient-stimulated echo with self-compensating gradient schemes and spin lock) sequence [20] with convection compensation [52]. Each experiment was repeated at least three times. Samples were prepared in buffer A with 100 % ^2H_2O. Dioxan was added to the samples as an internal diffusion standard [21]. The diffusion delay and the coding gradient pulse width were 100 and 4 ms respectively.

Diffusion data (signal intensity versus gradient strength) were fitted to Gaussian functions with Kaleidagraph 3.6 (Synergy Software, Reading, PA, U.S.A.). The Stokes radii of the polypeptides were calculated from the apparent diffusion coefficients of dioxan and of the polypeptide, and the known Stokes radius of dioxan (2.12 Å, where 1 Å $= 10^{-10}$ m, see [21]).

CD

CD spectra were recorded using an AVIV CDS 215 spectropolarimeter. Spectra were obtained at 21 °C with polypeptide samples in buffer A prepared without ^2H_2O. Polypeptide concentration was determined by absorption spectroscopy using the Edelhoc method and the molar absorption coefficients published by Pace and co-workers [22]. Spectra were recorded with a step of 0.5 nm, a constant bandwidth of 1.0 nm and 2.0 s of integration time.

In the near-UV region (250–350 nm), the optical path was 1.0 cm and the concentrations of KAaH1 and KAaH2 were 0.33 and 0.27 mg/ml respectively. In the far-UV region (180–260 nm), spectra were acquired with an optical path of 0.02 cm using circular cells and a concentration of 0.3 mg/ml for KAaH1 and of 0.54 mg/ml for KAaH2. Each spectrum corresponds to the accumulation of five scans.

Quantitative secondary structure composition was determined from the far-UV polypeptide spectra after normalization using the algorithm CONTIN [23] as implemented in the CD-Pro software [24], and the method of variable selection of spectra from the database [25].

Sequence comparison

Proteins showing sequence similarity with KAaH1 and KAaH2 were identified with BLAST2 [26] on the Universal Protein Resource (version 1.6) database. Best hits were scorpion toxins. A representative set of sequences was selected for several types of scorpion toxins for alignment with CLUSTAL W [27].

Molecular modelling

A model of the structure of KAaH1, KAaH2, birtoxin and ikitoxin was obtained by homology modelling with the program Modeller 6v2 [28]. Homologous polypeptides with known structure were identified by a BLAST2 [26] search of the Protein Databank database (RCSB organization) using the KAaH1 sequence. Six scorpion toxins with a BLAST2 expectancy value lower than 0.0007 were selected (Protein Databank codes 1SN1 [29], 1LQQ [30], 1NRA [31], 1CN2 [32], 1B3C [33] and 1VNA [34]). A multiple sequence alignment was obtained from a structure multiple alignment using the CE software [35,36]. The output alignment from CE was then aligned with KAaH1 and KAaH2, using CLUSTAL W [27]. The resulting alignment and the corresponding structures were used as input for Modeller. For each model, 20 structures were calculated. Their stereochemical properties were analysed with PROCHECK 3.5.4 [37].

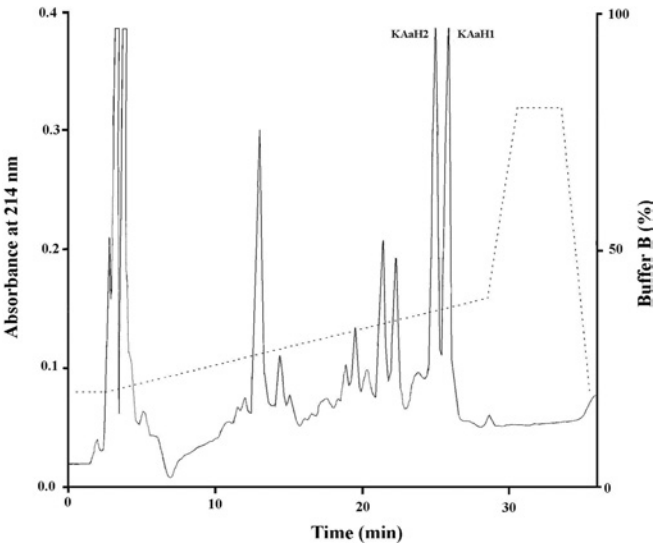

Figure 1 Purification of KAaH1 and KAaH2

The toxic fraction of the venom was submitted to FPLC on a Mono S column. KAaH1 and KAaH2 were purified from the non-retained fraction by RP-HPLC on a C8 column using a gradient of solution B (0.1 % TFA in acetonitrile) as described in the Experimental section. KAaH1 and KAaH2 were collected at 24.30 and 23.93 min respectively.

RESULTS

Purification of KAaH1 and KAaH2

The toxic fraction obtained from Sephadex G-50 chromatography of the venom was fractionated on a Mono S column. The non-retained fraction was injected into a C8 column (Figure 1). KAaH1 and KAaH2 were eluted at 24.30 and 23.93 min respectively. An analytical HPLC run of the fractions corresponding to each of the polypeptides showed a single symmetric peak. KAaH1 and KAaH2 represent about 10 % of the AaHG50 toxic fraction each. Injection of KAaH1 or KAaH2 into mice induced no toxic symptoms up to 2 μg doses.

Electrophysiological characterization

The inhibitory effect of KAaH1 (100 nM) was studied on *X. laevis* oocytes expressing Kv1.1 channels, which are only present in the central nervous system, or Kv1.3 channels, which are known to be essential for lymphocyte proliferation. Kv1.1 channels show a higher current inhibition (92 %) than Kv1.3 (62 %), with the same KAaH1 concentration (Figure 2A). At each concentration (0.5, 1, 5, 10, 20, 50 and 100 nM) and in the -40 to $+40$ mV range, the blocking potency of KAaH1 slightly increased with the pulse level. The blocking potency of KAaH1 was assessed by measuring the current remaining after stepwise increases in KAaH1 concentration from 0.5 to 100 nM. Fitting of the dose–response data to hyperbolic curves gave IC_{50} values of 5.3 ± 0.1 and 50.0 ± 0.1 nM for Kv1.1 and Kv1.3 channels respectively (Figure 2B).

The activity of KAaH2 on Kv1.1 (Figure 2C) and Kv1.3 currents (results not shown) was also studied. KAaH2 showed a weak

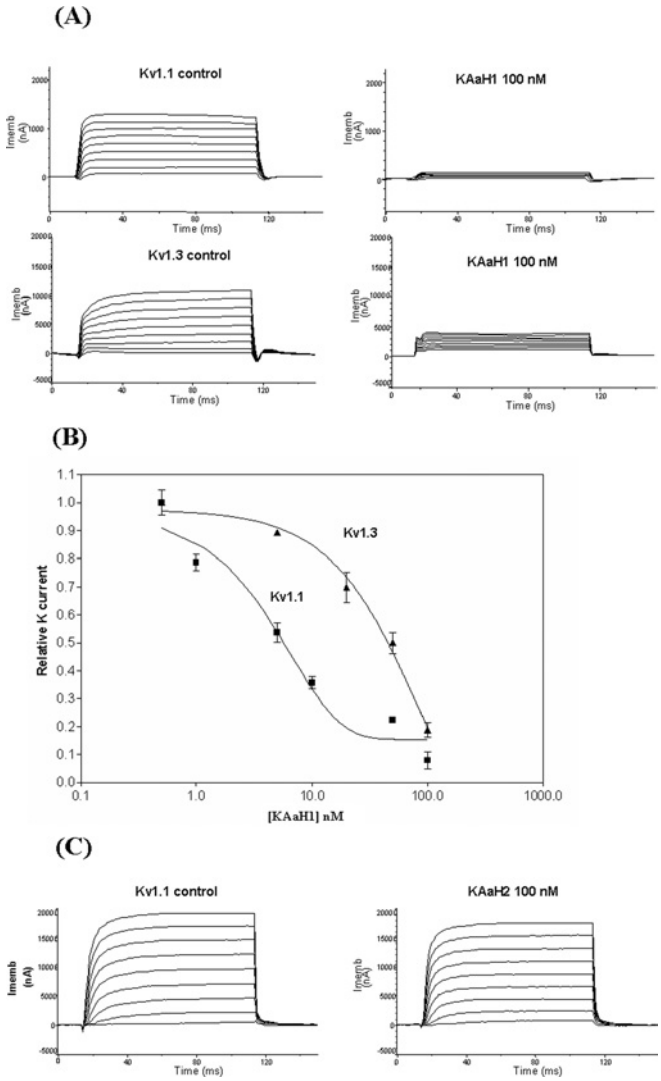

Figure 2 Effect of KAaH1 and KAaH2 on K^+ channels

Superimposed currents induced by 100 ms depolarizing pulses from –40 to +40 mV, in 10 mV steps. The holding potential was –80 mV. Leak and capacitive currents were subtracted. (**A**) Blockade of Kv1.1 and Kv1.3 currents by 100 nM KAaH1. (**B**) Dose–response curves on Kv1.1 and Kv1.3 channels. Results are means ± S.E.M. for 3–7 separate experiments. Results are expressed as the relative current persisting in the presence of the toxin. (**C**) Blockade of Kv1.1 currents by 100 nM KAaH2. The left panels labelled 'control', correspond to channel currents in the absence of KAaH1 and KAaH2. Imemb, current inhibition.

(20 %) and not sustained K^+ current inhibition at 100 nM concentration. This polypeptide showed no activity on Kv1.3 channels up to 100 nM concentration.

In addition to a classical blockade on Kv1.1 and Kv1.3 currents observed for K^+ channel toxins, an unexpected behaviour was observed. Indeed, at each concentration, and in a dose-independent manner, KAaH1 blockade showed a lag time before the beginning of a continuous and progressive inhibition. During this time, currents showed an irregular and slight amplitude fluctuation. The duration of this lag phase was unrelated to the time needed to reach the maximum blockade for each toxin concentration.

The effects of KAaH1 and KAaH2 on voltage-dependent Na^+ channels were studied by means of whole-cell patch–clamp recordings of tsA-201 cells transfected with Nav1.2a, a major Na^+ channel subunit expressed in the brain, or Nav1.5, the major cardiac isoform.

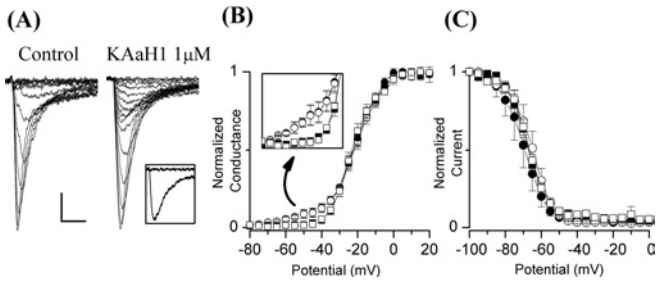

Figure 3 Effects of KAaH1 and KAaH2 on voltage-gated Na^+ channels

(**A**) Representative Nav1.2a current traces recorded in control conditions and with 1 μM KAaH1. Currents were elicited with depolarizing pulses from –75 to –10 mV in 5 mV steps, and a holding potential of –100 mV. Scale bars: 600 pA, 1 ms for the traces on the left; 1000 pA, 1 ms for the traces on the right. Inset: superimposed currents recorded with a depolarizing step to –45 mV, in control and with 1 μM KAaH1, shown to highlight the effects of the toxin. (**B**) Activation curve in control conditions (□, $n=6$), in control conditions with the depolarizing prepulse (■, $n=6$), with 1 μM KAaH1 (○, $n=4$), and with 1 μM KAaH1 and the depolarizing prepulse (●, $n=4$). The inset is a magnification of the points between –80 and –30 mV. (**C**) Inactivation curve for the four above conditions ($n=6$ in control, $n=4$ with KAaH1).

To assess the effect of KAaH1 on Nav1.2a, Na^+ currents were recorded during perfusion with KAaH1 at the concentration of 100 nM. KAaH1 did not have any effect on current amplitude or kinetics, or on the voltage dependence of activation and inactivation (results not shown). However, as is well-documented in the literature, the shift of the voltage dependence of activation characteristically produced by β scorpion toxins is elicited by short prepulses to positive potentials (see for instance [38]). Thus KAaH1 was also tested with this stimulation method (see the Experimental section) but no significant effects were observed.

KAaH1 was also tested at 1 μM, adding the toxin to the extracellular bath solution. The kinetics of the current was the same as in the control, but the current was activated at more negative potentials (Figure 3A). In fact, KAaH1 induced a partial negative shift in the voltage dependence of activation (Figure 3B; parameters of the Boltzmann fits: control, $Va=-22.4\pm0.5$, $k=6.9\pm0.2$; KAaH1, double Boltzmann, $A_1=0.10\pm0.03$, $Va_1=-55\pm1$, $k_1=15\pm4$, $A_2=0.90\pm0.02$, $Va_2=-20.9\pm0.7$, $k_2=7.0\pm0.5$). Interestingly, this effect was prepulse-independent (Figure 3B; control, $Va=-21.9\pm0.4$, $k=7.0\pm0.2$; KAaH1, $A_1=0.12\pm0.02$, $Va_1=-51\pm1$, $k_1=18\pm5$, $A_2=0.88\pm0.02$, $Va_2=-20.2\pm0.5$, $k_2=7.2\pm0.4$) and the voltage dependence of inactivation was not significantly modified (Figure 3C).

KAaH1 did not have any significant effect on Nav1.5 when perfused at a concentration of 100 nM ($n=3$, not shown). When added to the extracellular bath solution (1 μM), KAaH1 did not alter the kinetics of Na^+ currents, did not induce any shift of the voltage dependence of activation and had no influence on the voltage dependence of inactivation (results not shown).

Similar results were observed for KAaH2 (results not shown), which was studied using the same experimental methods. Indeed, KAaH2 (1 μM) induced a partial prepulse-independent negative shift of the voltage dependence of activation of Nav1.2a Na^+ channels, whereas no effects were observed with a 100 nM concentration. KAaH2 did not have any significant effects on Nav1.5 at the concentrations of 100 nM and 1 μM.

Sequence determination and comparison with other scorpion toxins

Edman degradation of 2 nmol of S-pyridyl-ethylated peptides led to the identification of the complete amino acid sequence of the peptides (Figure 4A). Both peptides are 58 residues long and

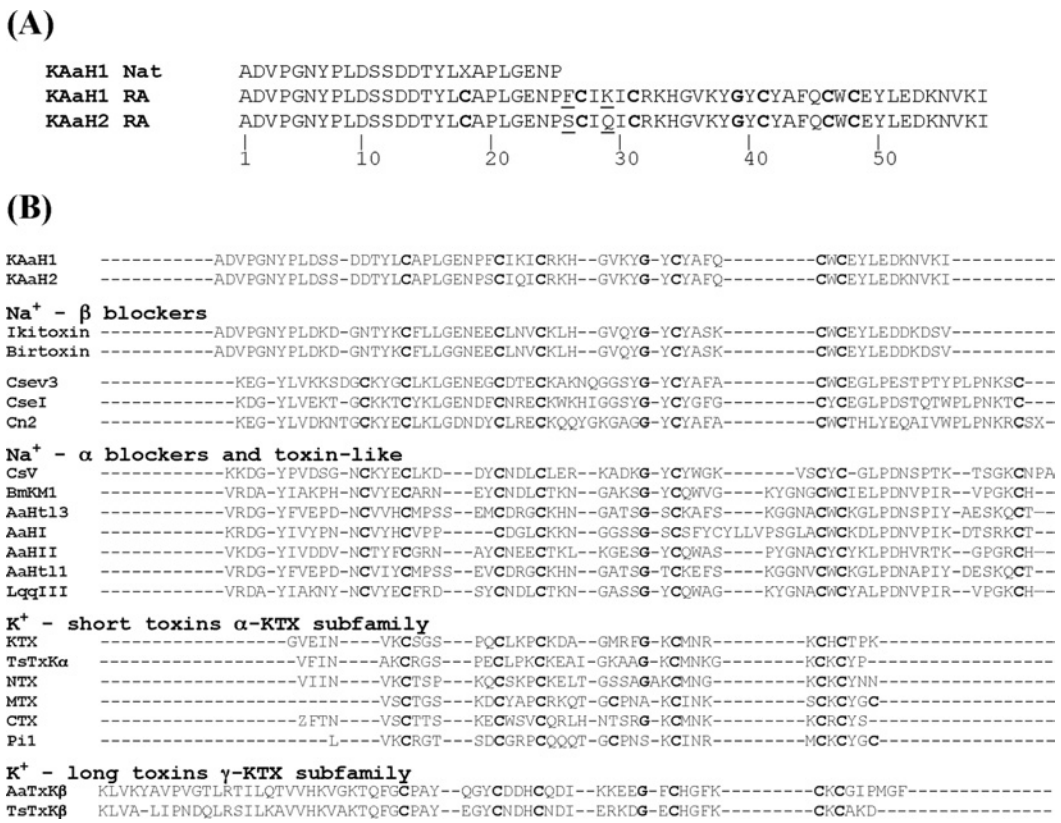

Figure 4 Amino acid sequence of KAaH1 and KAaH2, and comparison with other scorpion toxins

(**A**) Amino acid sequence determination of native KAaH1 (KAaH1 Nat), and of reduced and alkylated KAaH1 (KAaH1 RA) and KAaH2 (KAaH2 RA). The residues that are different in KAaH1 and KAaH2 are underlined. (**B**) Sequence comparison of KAaH1 and KAaH2 with toxins active against Na^+ channel [6,10,11,29–32,34,42,43], and toxins active against various sub-types of K^+ channels [40,44–50]. The alignment was obtained with CLUSTAL W as described in the Experimental section. A gap was introduced manually in Na^+ α-neurotoxins sequences to align the C-terminal cysteine with that of long Na^+ β-toxins. Cysteines and the conserved glycine residue are highlighted.

contain six cysteines. The experimental masses of native KAaH1 (6652.15 ± 0.67 Da) and KAaH2 (6592.5 ± 0.19 Da) obtained by electrospray ionization techniques, are effectively identical with the average masses calculated from the corresponding sequence for the fully oxidized form: 6652.59 Da for KAaH1 and 6592.44 Da for KAaH2. Moreover, only a monomeric form was observed in the mass spectra of both polypeptides, suggesting that no intermolecular disulphide bridge is formed. These results indicate that the six cysteines of KAaH1 and KAaH2 are engaged in three intramolecular disulphide bridges.

The sequences of KAaH1 and KAaH2 are very similar. Indeed, they only show two different amino acids at positions 26 (Phe/Ser) and 29 (Lys/Gln) (Figure 4A). Both polypeptides show a high level of identity with birtoxin and ikitoxin ($\sim$60 %), two 58 residues scorpion toxins that block mammal Na^+ channels and whose sequences only differ by one amino acid (Gly/Glu at position 23).

Compared with other scorpion toxins, KAaH1 and KAaH2 show the highest similarity ($\sim$46–48 % over 58 residues) with β-type Na^+ channel toxins, and then with α-type Na^+ channel toxins ($\sim$29–36 % over 58 residues) (see Figure 4B). The lowest similarity is observed with short and long scorpion toxins active on K^+ channels (23–42 % over 34–39 residues and $\sim$25 % over $\sim$50 residues respectively). The alignment of KAaH1 and KAaH2 cysteine residues with those of all the sequences displayed in Figure 4(B), strongly indicates that both polypeptides show the typical pairing of half-cysteines observed in scorpion toxins (C-1 with C-4, C-2 with C-5 and C-3 with C-6).

NMR

The structures of KAaH1 and KAaH2 were characterized by homonuclear ^{1}H-NMR. The spectra of both polypeptides show broad lines and a low number of cross-peaks at temperatures between 5 and 35 °C and at ^{1}H resonance frequencies of approx. 500 and 600 MHz. This can be observed in the spectra of KAaH1 obtained at 15 °C, the temperature at which the spectra were of better quality (Figure 5). For instance, in the purged COSY experiment, which is very sensitive to broad lines, only three cross-peaks between amide (7–9 p.p.m.) and Hα protons (4–6 p.p.m.) are observed, instead of the approx. 57 correlations that are expected (KAaH1 has 58 residues, four prolines and four glycines). In addition, in the TOCSY spectrum, only 25 cross-peaks between amide and Hα protons are observed and there are only few correlations between amide protons and side-chains. A detailed comparison of NOESY and TOCSY spectra, both recorded in H_2O and in ^2H_2O, indicated that NOESY spectra contain mainly intra-residue correlations and may contain only a few 'long-distance' interactions. In an attempt to obtain sharper lines, the pH of a sample of both polypeptides (pH 6.5 instead of pH 4.0) and the ionic strength (up to 50 mM sodium phosphate and 200 mM NaCl) were varied. However, the lines remained broad and the spectra of poor quality.

The broad lines and the resulting lack of cross-peaks in the spectra of both polypeptides hamper the assignment of the signals and the determination of the polypeptide structures. Some

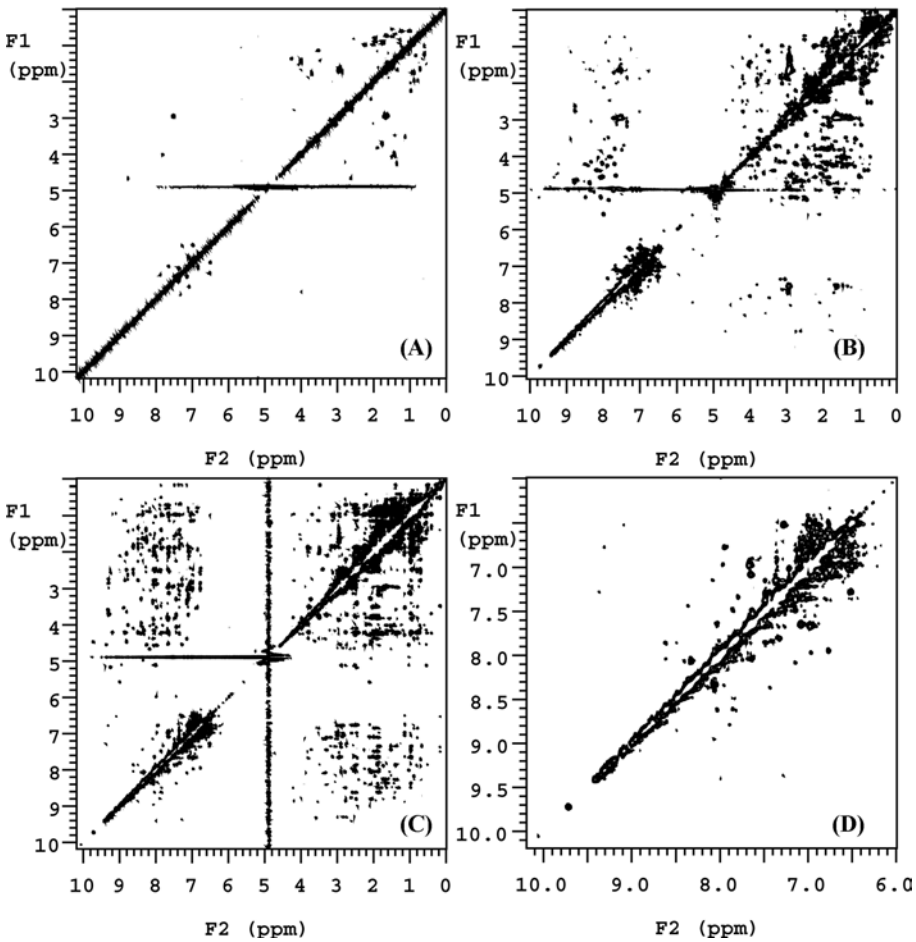

Figure 5 ^{1}H- NMR two-dimensional spectra of KAaH1

Purged COSY (**A**), TOCSY (**B**) and NOESY (**C**) spectra. (**D**) High-field region of the NOESY spectrum. The spectra were obtained at 15 °C as described in the Experimental section.

structural information, however, can be obtained from the qualitative analysis of the spectra. First, although the spectra of KAaH1 and KAaH2 show some differences (results not shown), these are similar, which suggests that they have a similar structure. Without resonance assignment, however, it is not possible to know if the differences in the spectra are due to the differences in the sequence (two residues), in the structure and/or in the dynamics of both polypeptides. Secondly, the spectra show good dispersion of chemical shifts, indicating that both polypeptides have, at least in some region, a tertiary structure. Thirdly, the fact that the spectra show downfield-shifted NH ($\delta > 8.7$ p.p.m.) and Hα ($\delta > 5.0$ p.p.m.) resonances, strongly suggests that the polypeptides contain β-sheet structures. Finally, the existence of NH–NH correlations (Figure 5D) may indicate the presence of turn like or α-helical structures, although the NH–NH correlations do not seem to be sequential, as normally observed for α-helices.

The broadening of the lines of both polypeptides relative to what is expected for a polypeptide of 58 residues may be due to one of the following reasons: (i) an abnormally high viscosity of the sample, (ii) oligomerization and (iii) exchange broadening due to conformational exchange at intermediate rate on the chemical shift time scale, that is in the millisecond time range. These three phenomena can indeed shorten the transversal relaxation time of proton magnetization and thereby cause broad lines. To distinguish between these possibilities, self-diffusion experiments of KAaH1 and KAaH2 were performed by pulse field-gradient NMR using dioxan, a molecule of known Stokes radius, as an internal standard. That dioxan in the presence or absence of KAaH1 and KAaH2 showed a very similar diffusion coefficient allows us to rule out viscosity as the cause of the broad lines. The Stokes radii of KAaH1 (16.4 ± 0.5 Å) and KAaH2 (16.7 ± 0.5 Å) were determined from the dependence of the intensity of the polypeptide and dioxan signals on the strength of the field gradients. These values are similar to the predicted value (from published results by Wilkins et al. [21]) for the Stokes radius of a monomeric polypeptide of the same size (58 residues) in its native (globular and compact) state: 15.4 Å. This observation indicates that both polypeptides are globular, compact and essentially monomeric under the conditions used in NMR experiments. Mainly, the diffusion results indicate that neither KAaH1 nor KAaH2 form well-populated oligomers of relatively high molecular mass that could lead to broadened NMR lines. Hence the broad lines observed for both polypeptides are due to conformational exchange and reveal motions of both polypeptide structures at the millisecond time scale.

CD

KAaH1 and KAaH2 contain six tyrosine residues and one tryptophan residue. The CD spectra of KAaH1 and KAaH2 in the

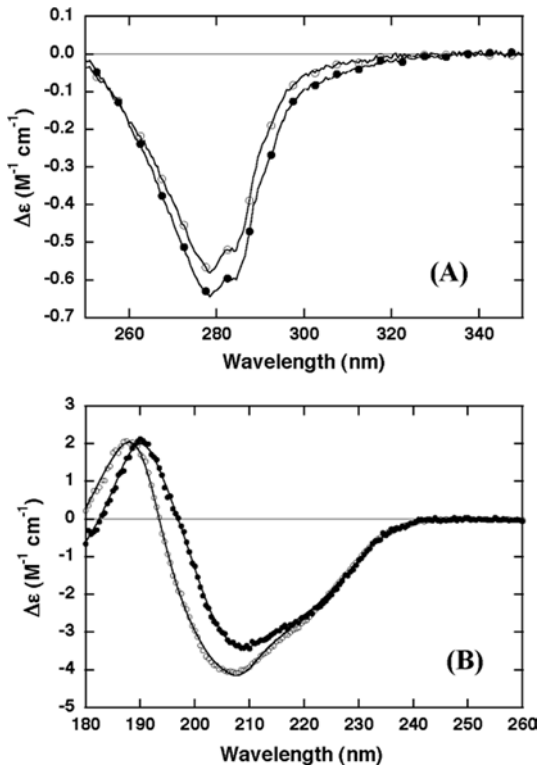

Figure 6 Near- and far-UV CD spectra of KAaH1 (●) and KAaH2 (○)

Spectra were acquired at 21 °C with the polypeptides dissolved in 10 mM deuterated sodium acetate pH 4.0. Far- (**A**) and near-UV (**B**) spectra were normalized taking into account the concentration of residues or of aromatic residues respectively. Solid lines in (**B**) correspond to the spectra obtained by quantitative analysis of the secondary structure using the CONTIN algorithm [23] in the CD-Pro software [24]. The root-mean-squared deviation between the experimental and predicted spectra is 0.06 for both polypeptides.

near-UV region show negative bands with two minima at 278.5 and 284.0 nm, which are characteristic of tyrosine residue absorption (Figure 6A). The spectra are thus dominated by the dichroism of tyrosine residues, indicating that at least one of the tyrosine residues is in an asymmetric environment. This result, and the good dispersion of chemical shifts in the NMR spectra of both polypeptides indicate that KAaH1 and KAaH2 show, at least partially, a fixed tertiary structure. It is to note that the CD spectra in the near-UV region do not show peaks at the absorption wavelengths of tryptophan residues (280 and 288 nm), which indicates that the aromatic ring of the single tryptophan residue (Trp^{47}) is well exposed to the solvent. In agreement with this, the aromatic protons of Trp^{47} (Hε3, Hζ2, Hζ3 and Hη2), which could be assigned in the NMR spectra of KAaH1 and KAaH2, show 'random-coil' like chemical shifts.

The far-UV CD spectra of KAaH1 and KAaH2 display a positive maximum at approx. 186–192 nm and a negative minimum at approx. 204–210 nm (Figure 6B). The quantitative deconvolution of the spectra in terms of secondary structure indicates that, at pH 4.0, both polypeptides contain approx. 16–17 % of α-helices and approx. 22–26 % of β-sheets. Far-UV spectra were also recorded in 10 mM potassium phosphate buffer at pH 6.5, which is closer to the physiological pH (results not shown). Although the spectra show differences with the spectra of the corresponding polypeptide at pH 4.0, the structural deconvolution does not show any significant difference in α-helical or β-sheet content.

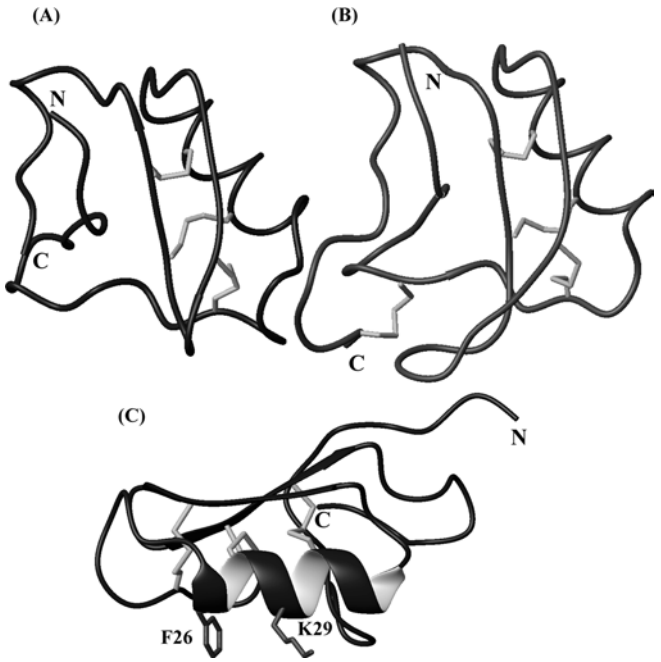

Figure 7 Homology models

(**A**) Backbone ribbon representation of the model of KAaH1 and (**B**) of the structure of neurotoxin BMK M1 (Protein Databank code 1SN1), which is one of the six structures used as a template. The side-chain bonds of cysteines and the disulfide bridges are indicated in light grey. In (**A**), the three N-terminal residues of KAaH1 are not shown. (**C**) Ribbon diagram of the model of KAaH1 showing the side chains of residues Phe^{26} and Lys^{29} in close proximity. This Figure was produced with MOLMOL 2k.1 [51].

Models of KAaH1 and KAaH2

The models of KAaH1, KAaH2, birtoxin and ikitoxin were established by homology modelling using as templates six structures of long toxins active on Na^+ channels. The models show good stereochemistry as analysed with PROCHECK [37]. Indeed, approx. 86 % of residues are in allowed regions and approx. 12 % in additionally allowed regions of the Ramachandran plot. Homology models of the four polypeptides are very similar, with a C_α root-mean-squared deviation lower than 1.5 Å for 58 residues.

The model of KAaH1 with the structure of the neurotoxin BMK M1 used as one of the template structures is shown in Figure 7. The models show the basic characteristics of the α/β-fold of scorpion toxins: three disulphide bridges (which were not introduced as constraints), a long α-helix (residues 25–34 for KAaH1 model) and an antiparallel β-sheet (residues 38–41 and 46–49 for KAaH1 model). The N- and C-terminal regions are close to each other, as observed in a model previously established for birtoxin [10]. Mainly, the secondary structure content of KAaH1 and KAaH2 calculated from the models (17 % of α-helix and β-sheet) are in close agreement with the CD data ($\sim$16–17 % of α-helix and $\sim$22–26 % of β-sheet), and the aromatic ring of Trp^{47} in the models is exposed to the solvent as shown by CD and NMR.

DISCUSSION

We have described the isolation and characterization of a new type of scorpion polypeptides from AaH scorpion venom: KAaH1 and KAaH2. These small proteins are 58 residues long, are cross-linked by three disulphide bridges and their sequences differ only at two positions. KAaH1 is active on voltage-gated Kv1 K^+ channels, and shows only very minor effects on brain Nav1.2a and no

effect on heart Nav1.5 Na^+ channels, whereas KAaH2 is barely active on the tested K^+ and Na^+ channels. The important sequence differences observed with respect to the members of the three major subfamilies of K^+-channel toxins, named α-KTx (see Figure 4), β-KTx (results not shown) and γ-KTx (see Figure 4) [39], as well as the activity of KAaH1, suggest that KAaH1 and KAaH2 should belong to a new subfamily of K^+-channel toxins.

Interestingly, the sequences of KAaH1 and KAaH2 are closer to scorpion toxins active on Na^+ channels as compared with toxins active on K^+ channels. The close similarity (67–69 % similarity) between the sequences of KAaH1 and KAaH2 and the β-type Na^+-channel blockers birtoxin and ikitoxin (58 residues, three disulphide bridges), suggests that these polypeptides belong to the same phylogenetic group, although these target quite different channels. Ikitoxin differs from birtoxin by one amino acid at position 23 (Glu/Gly) and has a much lower activity on goldfish Na^+ channels compared with birtoxin [11]. Like ikitoxin, KAaH1 and KAaH2 contain a glutamine residue at position 23. The very weak activity of KAaH1 and KAaH2 on Nav1.2a Na^+ channels and their lack of activity on Nav1.5 channels may be due, at least in part, to the presence of this negatively charged residue at position 23. The net negative charge of the N-terminal region (residues 10–18) of KAaH1 and KAaH2 may also be relevant to the low activity that these polypeptides show towards the tested Na^+ channels.

KAaH2 differs from KAaH1 by only two amino acids at positions 26 (Ser/Phe) and 29 (Gln/Lys). These differences, however, have a drastic effect on the activity of these proteins on Kv1.1 and Kv1.3 channels. Indeed, KAaH1 blocks Kv1.1 and Kv1.3 currents with an IC_{50} value of 5 and 50 nM respectively, whereas KAaH2 blocks only 20 % of Kv1.1 currents and is not active on Kv1.3 channels at a concentration of 100 nM. These results indicate the importance of Lys^{26} and/or Phe^{29} on the affinity of KAaH1 to these voltage-gated K^+ channels.

Short and long scorpion toxins usually give ^{1}H-NMR spectra with sharp lines and very good signal dispersion that are readily amenable to resonance assignment and structure determination. Unexpectedly, under several experimental conditions, the two-dimensional ^{1}H-spectra of KAaH1 and KAaH2 showed relatively few resonances and broad lines that hampered signal assignment. Analysis of the spectra indicated, however, that the two polypeptides contain β-sheet and probably α-helical structures, and at least in some region of the molecule, a fixed tertiary structure. In addition, the superposition of many resonances in the NOESY spectra of KAaH1 and KAaH2 suggests that the polypeptides may have a similar structure. CD results are in agreement with these observations. Indeed, deconvolution of the CD spectra in the far-UV region indicated that both polypeptides contain roughly 17 % of α-helices and 24 % of β-sheets. Moreover, in the near-UV region, these polypeptides show CD characteristic of tyrosine residues, indicating, like the good dispersion of resonances in NMR spectra, that at least some region of the polypeptides has a fixed tertiary structure.

Diffusion experiments were performed by NMR to assess whether the broad lines observed in ^{1}H spectra of both polypeptides were due to an abnormally high viscosity of the NMR samples, oligomerization or exchange broadening. These experiments allowed us to rule out the first two possibilities and indicated that the Stokes radii of both polypeptides (16.4 and 16.7 ± 0.5 Å for KAaH1 and KAaH2 respectively) are in agreement with both polypeptides being in a compact, globular and essentially monomeric state. Hence KAaH1 and KAaH2 show a conformational exchange at the millisecond time scale, and the broad lines observed in NMR are due to this phenomenon. It is important to note that this conformational exchange involves a substantial part of each molecule because many resonances are exchange-broadened.

We obtained a model of the structure of KAaH1 and KAaH2 based on the homology and high sequence similarity of these polypeptides with Na^+ channel toxins of known structure. In addition to the high sequence similarity, the models are supported by the perfect alignment of cysteine residues of both polypeptides with those of all other known scorpion toxins, and are in accordance with experimental results. In particular, the secondary-structure content obtained from the models and from CD data are effectively the same; NMR spectra show that both polypeptides contain β-sheet and probably α-helical structures; diffusion data indicate that both polypeptides are in a globular compact state; MS indicates that KAaH1 and KAaH2 contain three disulphide bonds; and the single tryptophan residue (Trp^{47}) is exposed to the solvent in the models as observed by NMR and CD in the near-UV region. Although the models are in good agreement with available experimental data, these only provide plausible static pictures of the polypeptide structures that are, in fact, in conformational exchange on the millisecond time scale as evidenced by NMR. As KAaH1 and KAaH2 lack the fourth disulphide bridge that covalently links the N- and C-terminal regions in long scorpion toxins, and because in long Na^+ toxins the N- and C-terminal regions make extensive contacts that are not all available in the shorter KAaH1 and KAaH2, it is tempting to think that the conformational exchange takes place in these regions of the molecules.

The α-KTx scorpion toxins interact with K^+ Kv1 channels through their C-terminal β-sheet region. Several conserved residues have been implicated in this interaction. Among them, two residues, an aromatic (Tyr or Phe) and a lysine residue, are known as the functional dyad and are particularly important. The lysine residue blocks the mouth of the ionic pore and the aromatic residue makes hydrophobic interactions with hydrophobic channel residues. Originally shown by Dauplais and co-workers for a sea anemone toxin [40], it has been reported that equivalent residues are present in sea-anemone (BgK), snake (dendrotoxin) and marine-cone snail (κ-PVIIA) toxins that display quite different scaffolds but recognize Kv1 channels (reviewed in [41]). These residues are very important for the interaction with K^+ channels and superimpose very well in the structures of the latter toxins from different organisms. Interestingly, two equivalent residues (Phe^{26} and Lys^{29}) are present in KAaH1 and absent in KAaH2, and these residues are relevant for the interaction with K^+ Kv1 channels (see above). In the model of KAaH1, the side-chains of Phe^{26} and Lys^{29} are located in the α-helix (Figure 7C). These side-chains are well exposed to the solvent and close to each other, showing several distances shorter than 7 Å, which is in good agreement with the distance of 6.6 ± 1.0 Å reported by Dauplais and co-workers [40] for sea-anemone BgK and α-KTx scorpion toxins. Taken together, the data presented in the present study pinpoint the latter residues as the functional dyad in KAaH1 and indicate that this polypeptide interacts with Kv1 K^+ channels by its α-helix side in contrast with short scorpion toxins of the α-KTx subfamily that use their β-sheet side.

In conclusion, KAaH1 and KAaH2 are the first members of a new subfamily of scorpion toxins related to Na^+ toxins in terms of sequence, but displaying a weak activity as β-type Na^+-channel modulators, probably due to their acidic N-terminal region. In contrast, KAaH1 efficiently blocks Kv1.1 and Kv1.3 channels, whereas KAaH2 is poorly active on Kv1.1 and inactive on Kv1.3 channels. Investigation of KAaH1 and KAaH2, which can be seen as natural mutants of the same polypeptide, led us to identify the putative functional dyad Lys^{26}/Phe^{29} of KAaH1, which is located in its α-helix and is very important for the activity on Kv1 channels.

We thank Professor A. L. Harvey, Dr L. Young (Department of Physiology and Pharmacology and Strathclyde Institute for Drug Research, University of Strathclyde, Glasgow, U.K.), Dr M.-F. Martin-Eauclaire, Dr S. Cestèle (Laboratoire d'Ingénierie des Proteines, Faculté de Médecine de Marseille, France), Professor G. Avanzini and Dr S. Franceschetti (Dipartimento di Neurofisiopatologia, Istituto Neurologico Besta, Milano, Italy) for their support. We also thank P. Lenormand and J.-C. Rousselle (Plateforme de Protéomique, Institut Pasteur, Paris, France) for MS of samples used for structural analysis. Professor K. Dellagi, Head of the Institut Pasteur of Tunisia, as well as Dr Z. Belasfar are acknowledged for their helpful advice. The 600 MHz NMR spectrometer was funded by the Région Ile de France and the Institut Pasteur.

REFERENCES

1 Miranda, F., Kopeyan, C., Rochat, H., Rochat, C. and Lissitzky, S. (1970) Purification of animal neurotoxins. Isolation and characterization of eleven neurotoxins from the venoms of the scorpions *Androctonus australis* Hector, *Buthus occitanus tunetanus* and *Leiurus quinquestriatus quinquestriatus*. Eur. J. Biochem. **16**, 514–523

2 Martin, M. F. and Rochat, H. (1986) Large scale purification of toxins from the venom of the scorpion *Androctonus australis* Hector. Toxicon **24**, 1131–1139

3 Zlotkin, E., Miranda, F. and Rochat, H. (1978) Chemistry and pharmacology of Buthinae scorpion venoms. In Handbook of Experimental Physiology, vol. 48 (Bettini, S., ed.), pp. 317–369, Springer-Verlag, Heidelberg

4 Possani, L. D. (1984) Structure of scorpion toxins. In Handbook of Natural Toxins, vol. 2 (Tu, A. T., ed.), pp. 513–550, Marcel Dekker, New York

5 Blanc, E., Hassani, O., Meunier, S., Mansuelle, P., Sampieri, F., Rochat, H. and Darbon, H. (1997) ^{1}H-NMR-derived secondary structure and overall fold of a natural anatoxin from the scorpion *Androctonus australis* Hector. Eur. J. Biochem. **247**, 1118–1126

6 Srairi-Abid, N., Mansuelle, P., Mejri, T., Karoui, H., Rochat, H., Sampieri, F. and El Ayeb, M. (2000) Purification, characterization and molecular modelling of two toxin-like proteins from the *Androctonus australis* Hector venom. Eur. J. Biochem. **267**, 5614–5620

7 Martin-Eauclaire, M. F. and Couraud, F. (1995) Scorpion neurotoxins: effects and mechanisms. In Handbook of Neurotoxicology, vol. 36 (Chang, L. W. and Dyer, R. S., eds.), pp. 683–716, Marcel Dekker, New York

8 Couraud, F., Jover, E., Dubois, J. M. and Rochat, H. (1982) Two types of scorpion receptor sites, one related to the activation, the other to the inactivation of the action potential sodium channel. Toxicon **20**, 9–16

9 Bontems, F., Roumestand, C., Gilquin, B., Ménez, A. and Toma, F. (1991) Refined structure of charybdotoxin: common motifs in scorpion toxins and insect defensins. Science **254**, 1521–1523

10 Inceoglu, B., Lango, J., Wu, J., Hawkins, P., Southern, J. and Hammock, B. D. (2001) Isolation and characterization of a novel type of neurotoxic peptide from the venom of the South African scorpion *Parabuthus transvaalicus* (Buthidae). Eur. J. Biochem. **268**, 5407–5413

11 Inceoglu, A. B., Hayashida, Y., Lango, J., Ishida, A. T. and Hammock, B. D. (2002) A single charged surface residue modifies the activity of ikitoxin, a β-type Na^+ channel toxin from *Parabuthus transvaalicus*. Eur. J. Biochem. **269**, 5369–5376

12 Johnson, B. A. and Blevins, R. A. (1994) NMRView: a computer program for the visualisation and analysis of NMR data. J. Biomol. NMR **4**, 603–614

13 Piotto, M., Saudek, V. and Sklenár, V. (1992) Gradient-tailored excitation for single-quantum NMR spectroscopy of aqueous solutions. J. Biomol. NMR **2**, 661–665

14 Liu, M. L., Mao, X.-A., Ye, C. H., Huang, H., Nicholson, J. K. and Lindon, J. C. (1998) Improved WATERGATE pulse sequences for solvent suppression in NMR spectroscopy. J. Magn. Reson. **132**, 125–129

15 Marion, D. and Bax, A. (1988) P.COSY, a sensitive alternative for double-quantum-filtered COSY. J. Magn. Reson. **80**, 528–533

16 Griesinger, C., Otting, G., Wüthrich, K. and Ernst, R. R. (1988) Clean Tocsy for ^{1}H spin system identification in macromolecules. J. Am. Chem. Soc. **110**, 7870–7872

17 Levitt, M. H., Freeman, R. and Frenkiel, T. (1982) Broadband heteronuclear decoupling. J. Magn. Reson. **47**, 328–330

18 Bax, A. and Davis, D. G. (1985) MLEV-17-based two-dimensional homonuclear magnetization transfer spectroscopy. J. Magn. Reson. **65**, 355–360

19 States, D. J., Haberkorn, R. A. and Ruben, D. J. (1982) A two dimensional nuclear Overhauser experiment with pure absorption phase in four quadrants. J. Magn. Reson. **48**, 286–292

20 Pelta, M. D., Barjat, H., Morris, G. A. and Davis, A. L. (1998) Pulse sequences for high-resolution diffusion-ordered spectroscopy (HR-DOSY). Magn. Reson. Chem. **36**, 706–714

21 Wilkins, D. K., Grimshaw, S. B., Receveur, V., Dobson, C. M., Jones, J. A. and Smith, L. J. (1999) Hydrodynamic radii of native and denatured proteins measured by pulse-field gradient NMR techniques. Biochemistry **38**, 16424–16431

22 Pace, C. N., Vajdos, F., Fee, L., Grimsley, G. and Gray, T. (1995) How to measure and predict the molar absorption coefficient of a protein. Protein Sci. **4**, 2411–2423

23 Provencher, S. W. and Glöckner, J. (1981) Estimation of globular protein secondary structure from circular dichroism. Biochemistry **20**, 33–37

24 Sreerama, N. and Woody, R. W. (2000) Estimation of protein secondary structure from circular dichroism spectra: comparison of CONTIN, SELCON, and CDSSTR methods with an expanded reference set. Anal. Biochem. **287**, 252–260

25 Manavalan, P. and Johnson, W. C. J. (1987) Variable selection method improves the prediction of protein secondary structure from circular dichroism spectra. Anal. Biochem. **167**, 76–85

26 Altschul, S. F., Madden, T. L., Schaffer, A. A., Zhang, J., Zhang, Z., Miller, W. and Lipman, D. J. (1997) Gapped BLAST and PSI-BLAST: a new generation of protein database search programs. Nucleic Acids Res. **25**, 3389–3402

27 Thompson, J. D., Higgins, D. G. and Gibson, T. J. (1994) CLUSTAL W: improving the sensitivity of progressive multiple sequence alignment through sequence weighting, positions-specific gap penalties and weight matrix choice. Nucleic Acids Res. **22**, 4673–4680

28 Sali, A. and Blundell, T. L. (1990) Definition of general topological equivalence in protein structures: a procedure involving comparison of properties and relationships through simulated annealing and dynamic programming. J. Mol. Biol. **212**, 403–428

29 He, X. L., Li, H. M., Zeng, Z. H., Liu, X. Q., Wang, M. and Wang, D. C. (1999) Crystal structures of two α-like scorpion toxins: non-proline *cis* peptide bonds and implications for new binding site selectivity on the sodium channel. J. Mol. Biol. **292**, 125–135

30 Landon, C., Cornet, B., Bonmatin, J. M., Kopeyan, C., Rochat, H., Vovelle, F. and Ptak, M. (1996) ^{1}H-NMR-derived secondary structure and the overall fold of the potent anti-mammal and anti-insect toxin III from the scorpion *Leiurus quinquestriatus quinquestriatus*. Eur. J. Biochem. **236**, 395–404

31 Jablonsky, M. J., Watt, D. D. and Krishna, N. R. (1995) Solution structure of an Old World-like neurotoxin from the venom of the New World scorpion *Centruroides sculpturatus* Ewing. J. Mol. Biol. **248**, 449–458

32 Pintar, A., Possani, L. D. and Delepierre, M. (1999) Solution structure of toxin 2 from *Centruroides noxius* Hoffmann, a β-scorpion neurotoxin acting on sodium channels. J. Mol. Biol. **287**, 359–367

33 Jablonsky, M. J., Jackson, P. L., Trent, J. O., Watt, D. D. and Krishna, N. R. (1999) Solution structure of β-neurotoxin from the New World scorpion *Centruroides sculpturatus* Ewing. Biochem. Biophys. Res. Commun. **254**, 406–412

34 Zhao, B., Carson, M., Ealick, S. E. and Bugg, C. E. (1992) Structure of scorpion toxin variant-3 at 1.2 Å resolution. J. Mol. Biol. **227**, 239–252

35 Shindyalov, I. N. and Bourne, P. E. (1998) Protein structure alignment by incremental combinatorial extension (CE) of the optimal path. Protein Eng. **11**, 739–747

36 Guda, C., Scheeff, E. D., Bourne, P. E. and Shindyalov, I. N. (2001) A new algorithm for the alignment of multiple protein structures using Monte Carlo optimization. Proc. Pacific Symp. Biocomp. **6**, 275–286

37 Laskowski, R. A., MacArthur, M. W., Moss, D. S. and Thornton, J. M. (1993) PROCHECK: a program to check the stereochemical quality of protein structures. J. Appl. Crystallogr. **26**, 283–291

38 Cestèle, S., Qu, Y., Rogers, J. C., Rochat, H., Scheuer, T. and Catterall, W. A. (1998) Voltage sensor-trapping: enhanced activation of sodium channels by beta-scorpion toxin bound to the S3-S4 loop in domain II. Neuron **21**, 419–431

39 Tytgat, J., Chandy, K. G., Garcia, M. L., Gutman, G. A., Martin-Eauclaire, M. F., van der Walt, J. J. and Possani, L. D. (1999) A unified nomenclature for short-chain peptides isolated from scorpion venoms: α-KTx molecular subfamilies. Trends Pharmacol. Sci. **20**, 444–447

40 Dauplais, M., Lecoq, A., Song, J., Cotton, J., Jamin, N., Gilquin, B., Roumestand, C., Vita, C., de Medeiros, C. L., Rowan, E. G. et al. (1997) On the convergent evolution of animal toxins. Conservation of a diad of functional residues in potassium channel-blocking toxins with unrelated structures. J. Biol. Chem. **272**, 4302–4309

41 Mouhat, S., Jouirou, B., Mosbah, A., De Waard, M. and Sabatier, J. M. (2004) Diversity of folds in animal toxins acting on ion channels. Biochem. J. **378**, 717–726

42 Rochat, H., Rochat, C., Miranda, F., Lissitzky, S. and Edman, P. (1970) The amino acid sequence of neurotoxin I of *Androctonus australis* Hector. Eur. J. Biochem. **17**, 262–266

43 Rochat, H., Rochat, C., Sampieri, F., Miranda, F. and Lissitzky, S. (1972) The amino-acid sequence of neurotoxin II of *Androctonus australis* Hector. Eur. J. Biochem. **28**, 381–388

44 Rogowski, R. S., Krueger, B. K., Collins, J. H. and Blaustein, M. P. (1994) Tityustoxin Kα blocks voltage-gated noninactivating K^+ channels and unblocks inactivating K^+ channels blocked by α-dendrotoxin in synaptosomes. Proc. Natl. Acad. Sci. U.S.A. **91**, 1475–1479

45 Legros, C., Ceard, B., Bougis, P. E. and Martin-Eauclaire, M. F. (1998) Evidence for a new class of scorpion toxins active against K^+ channels. FEBS Lett. **431**, 375–380

46 Gairi, M., Romi, R., Fernandez, I., Rochat, H., Martin-Eauclaire, M. F., Van Rietschoten, J., Pons, M. and Giralt, E. (1997) 3D structure of kaliotoxin: is residue 34 a key for channel selectivity? J. Pept. Sci. **3**, 314–319

47 Park, C. S. and Miller, C. (1992) Interaction of charybdotoxin with permeant ions inside the pore of a K^+ channel. Neuron **9**, 307–313

48 Olamendi-Portugal, T., Gómez-Lagunas, F., Gurrola, G. B. and Possani, L. D. (1996) A novel structural class of K^+-channel blocking toxin from the scorpion *Pandinus imperator*. Biochem. J. **315**, 977–981

49 Kharrat, R., Mansuelle, P., Sampieri, F., Crest, M., Oughideni, R., Van Rietschoten, J., Martin-Eauclaire, M. F., Rochat, H. and El Ayeb, M. (1997) Maurotoxin, a four disulfide bridge toxin from *Scorpio maurus* venom: purification, structure and action on potassium channels. FEBS Lett. **406**, 284–290

50 Sitges, M., Possani, L. D. and Bayon, A. (1986) Noxiustoxin, a short-chain toxin from the Mexican scorpion *Centruroides noxius*, induces transmitter release by blocking K^+ permeability. J. Neurosci. **6**, 1570–1574

51 Koradi, R., Billeter, M. and Wüthrich, K. (1996) MOLMOL: a program for display and analysis of macromolecular structures. J. Mol. Graph. **14**, 51–55

52 Jerschow, A. and Müller, N. (1997) Suppression of convection artifacts in stimulated-echo diffusion experiments. Double-stimulated-echo experiments. J. Magn. Reson. **125**, 372–375

Received 17 August 2004/16 December 2004; accepted 19 January 2005
Published as BJ Immediate Publication 19 January 2005, DOI 10.1042/BJ20041407